25th ABCM International Congress of Mechanical Engineering
October 20-25, 2019, Uberlândia, MG, Brazil

COB-2019-0213
NUMERICAL INVESTIGATION OF GAS-SOLID FLUIDIZED BEDS IN NARROW TUBES

Karlo Fernandes Rocha[a,b,1]
Fernando David Cúñez Benalcázar[a,2]
Erick de Moraes Franklin[a,3]
[a]University of Campinas, School of Mechanical Engineering, Rua Mendeleyev, 200, Campinas, 13083-860, Brazil
[b]Federal Institute of Espírito Santo, Rodovia BR-482 (Cachoeiro-Alegre), 29300-970, Cachoeiro de Itapemirim, ES, Brazil
[1]karlor@ifes.edu.br, [2]fernandodcb@fem.unicamp.br, [3]franklin@fem.unicamp.br

Abstract. *In this study, the behavior of gas-solid fluidized beds in narrow tubes is numerically investigated using an Eulerian-Lagrangian approach (CFD-DEM). The beds were formed in a vertical tube with a diameter of* $D = 2.5$ *mm and were filled with glass spheres with a diameter of* $d = 0.5$ *mm. Two different beds were arranged, consisting of 400 and 600 glass beads, and three air flows that correspond to cross-sectional mean velocities of* $\overline{U} = 1.05, \overline{U} = 1.10$ *and* $\overline{U} = 1.15$ *m/s were imposed at the bottom of the tube. Under these conditions, we observed the formation of alternating high- and low-compactness regions, known as plugs and piston bubbles, that propagate with characteristic lengths and celerities. The numerical simulations were performed using the open source codes CFDEM, OpenFOAM and LIGGGHTS. We tracked every single particle and the local volume fraction to obtain the main behavior of this problem. The collisional phenomena were studied and collision detection was based on the use of a peak acceleration to characterize particle-particle and particle-wall collision.*

Keywords: *fluidized bed, gas-solid, plugs, CFD-DEM, Eulerian-Lagrangian method.*

1. INTRODUCTION

Fluidized beds are extensively used in the chemical, pharmaceutical and mineral industry. It can be found in a wide range of applications such as coal burning, coal gasification, organic synthesis, mineral processing and incineration of waste. In the case of gas-solid fluidized beds, when the velocity of the fluid flow is increased to a certain value, the drag force exerted by the fluid balances with the weight of the particles, reaching thus the suspension of particles. This velocity is known as settling velocity at the inception of fluidization or minimum velocity of fluidization. At higher flow rates the bed may become unstable and part of the fluid passes through the bed in the form of bubbles or slugs. Bubbles occur in beds where the diameter of the tube is large when compared to their height and is characterized by regions of voids that propagate upwards along the bed, whereas plugs and piston bubbles occur in narrow diameter beds and are characterized by compact regions of high and low concentration of particles, respectively. This behavior can also occur in narrow SLFB (solid-liquid fluidized beds).

Gas-solid fluidized beds in wide channels and tubes are very unstable and rapidly reach a bubbling regime. Several studies investigated the instabilities appearing in gas fluidized beds (Tsuji *et al.*, 1992; Hoomans *et al.*, 1996; Zhou *et al.*, 2010; Goldschmidt *et al.*, 2002; Xu *et al.*, 2007; Wu *et al.*, 2013; Kafui *et al.*, 2002), however, no one studied the narrow case, where the ratio between the tube and the particles is $D/d < 10$.

Many studies have investigated the instabilities in the gas-solid system using an Eulerian-Eulerian numerical approach. In these simulations, the fluid and solid phases are considered as a continuous media and both can be solved by computational fluid dynamics (CFD), (Cammarata *et al.*, 2003; Mahinpey *et al.*, 2007; Hosseini *et al.*, 2009). Other studies in the literature have used an Eulerian-Lagrangian approach for the study of fluidized beds (Tsuji *et al.*, 1992; Hoomans *et al.*, 1996; Zhou *et al.*, 2010; Goldschmidt *et al.*, 2002) where the solid phase is considered as discrete and the fluid phase is considered as continuous. The solid phase, based on Discrete Element Method (DEM, citepcundall1979discrete), is solved by Newtion's second law of motion applied to a discrete system, while the fluid phase, based on (CFD), is solved by Navier Stokes equations. This approach is also known as CFD-DEM. In the last years, several studies (Tsuji *et al.*, 1992; Hoomans *et al.*, 1996; Zhou *et al.*, 2010) have demonstrated that CFD-DEM simulations can predict the hydrodynamics of fluidized beds well.

In the case of liquid fluidized beds, they are less unstable than gas fluidized beds and usually present a voidage-wave instability (Anderson and Jackson, 1969; Zenit and Hunt, 2000; Duru and Guazzelli, 2002; Aguilar-Corona *et al.*, 2011; Ghatage *et al.*, 2014). For the very narrow case, Cúñez and Franklin (2019), studied experimentally and numerically the

behavior of liquid fluidized beds, where the ratio between the tube and the particles was $D/d = 4.23$. The beds were formed in a tube with an internal diameter of D=25.4 mm and consisted of alumina particles with a diameter of $d = 6$ mm. With these conditions, the authors observed the formation of the granular plugs and piston bubbles. They also found that the characteristic lenghts of the plugs for this specific case were around 7 to 9 particle diameters.

A direct assessment of the collisional motion within a gas-solid flow was conducted in the present investigation. For that, we investigated a gas-solid fluidized bed. The particles are fluidized as the bed expands and in this state the particles have a significant agitation which is a caused by either collisions or hydrodynamic forces. Hence, particle-particle and particle-wall collisions are inherent of a fluidized bed description and influence the overall agitation level through the transport properties. The collisional phenomena were studied and collision detection was based on the use of a peak acceleration to characterize particle-particle and particle-wall collision (Aguilar-Corona *et al.*, 2011).

In this work, we investigate numerically the confinement effects in gas-solid fluidized beds of circular cross section. Depending on the ratio between the tube and the particles, such effects lead to the formation of alternating high- and low-compactness regions, known as plugs and piston bubbles, which have characteristic lengths and velocities. The gas-solid fluidized beds were formed in a 5 cm long vertical tube with a diameter of $D = 2.5$ mm and were filled with glass spheres with a diameter of $d = 0.5$ mm and density of $\rho_p = 2500$ kg/m^3. Thus, the ratio between the tube and the particles was $D/d = 5$. We computed the characteristic lengths and celerities of the plugs, the trajectories of individual grains, and the collisional statistics of grains for this specific case.

2. FORMULATION OF THE NUMERICAL MODEL

2.1 Governing equations

The mass and momentum equations for the gas phase are given respectively by

$$\frac{\partial \rho_f \varepsilon_f}{\partial t} + \nabla \cdot (\rho_f \varepsilon_f \vec{u}_f) = 0 \tag{1}$$

$$\frac{\partial \rho_f \varepsilon_f \vec{u}_f}{\partial t} + \nabla \cdot (\rho_f \varepsilon_f \vec{u}_f \vec{u}_f) = -\varepsilon_f \nabla P + \varepsilon_f \nabla \cdot \vec{\vec{\tau}} + \rho_f \varepsilon_f \vec{g} + \vec{F}_{p,f} \tag{2}$$

where P represent the pressure, $\vec{g}$ is the acceleration of gravity, $\vec{\vec{\tau}}$ is the stress tensor and $\rho_f, \varepsilon_f, \vec{u_f}$ are the density, volume fraction and mean velocity of the fluid, respectively. The last term $\vec{F}_{p,f}$ on the right represents the drag force per volume, is computed by Gidaspow model (Gidaspow, 1994) and given by

$$\vec{F}_{p,f} = \frac{1}{V_{cell}} \sum \vec{F}_d = \frac{1}{V_{cell}} \sum \frac{V_{p_i} \beta}{(1-\varepsilon_f)} (\vec{u}_f - \vec{u}_p) \tag{3}$$

where β is the coefficient of momentum transfer between phases due to the drag force, V_{cell} is the volume of each cell and V_{p_i} is the volume of particle i in cell. The coefficient β is given by

$$\beta = \begin{cases} 150 \dfrac{(1-\varepsilon_f)^2 \mu_f}{\varepsilon_f d_p^2} + 1.75 \dfrac{\rho_f |\vec{u}_f - \vec{u}_p| (1-\varepsilon_f)}{d_p}, & \varepsilon_f < 0.8 \\ \dfrac{3}{4} C_d \dfrac{\rho_f \varepsilon_f (1-\varepsilon_f) |\vec{u}_f - \vec{u}_p|}{d_p} \varepsilon_f^{-2.65}, & \varepsilon_f \geq 0.8 \end{cases} \tag{4}$$

where C_d is the drag coefficient and is related to the particle Reynolds number by

$$C_d = \begin{cases} \dfrac{24}{Re_p} \left(1 + 0.15 \left(Re_p\right)^{0.687}\right), & Re_p < 1000 \\ 0.44, & Re_p \geq 1000 \end{cases} \tag{5}$$

with

$$Re_p = \frac{\rho_f \varepsilon_f d_p |\vec{u}_f - \vec{u}_p|}{\mu_f}. \tag{6}$$

For the solid phase, the motion of each particle is calculated by linear and angular momentum equations and are given by

$$m_p \frac{d\vec{u}_p}{dt} = -V_p \nabla P + V_p \nabla \cdot \vec{\vec{\tau}} + m_p \vec{g} + \left[\sum_{i,j} \vec{F}_{c,i,j} + \sum_{i,w} \vec{F}_{c,i,w} \right] - V_p \vec{F}_{p,f} \tag{7}$$

$$I_p \frac{d\vec{\omega}}{dt} = \sum_{i,j} \vec{T}_{p,i,j} + \sum_{i,w} \vec{T}_{p,i,w} \tag{8}$$

where $\vec{u_p}$, m_p, V_p are the velocity, mass and volume of solid particle, respectively. T_p is the torque from the tangential component of the contact force, and I_p and $\vec{\omega}$ are the moment of inertia and angular velocity of a particle, respectively.

For particle-particle interactions, the spring-dashpot model is employed for the contact force $\vec{F}_{c,i,j} = \vec{F}_{cn,i,j} + \vec{F}_{ct,i,j}$ where $\vec{F}_{cn,i,j}$ and $\vec{F}_{ct,i,j}$ are normal and tangential components. The main equations of the spring-dashpot model are described in Cundall and Strack (1979).

2.2 Numerical setup

In the numerical simulations, we considered a gas-solid fluidized bed in a 5 cm long vertical tube with a diameter of $D = 2.5$ mm and filled with glass spheres with a diameter of $d = 0.5$ mm, and the fluid was air. Two different beds were arranged, consisting of 400 and 600 glass beads, and three air flows corresponding to cross-sectional mean velocities of $\overline{U} = 1.05$, $\overline{U} = 1.10$ and $\overline{U} = 1.15$ m/s were imposed at the tube inlet. Initially, the particles are randomly inserted to fall freely without air flow until they reach the bottom of the tube. After a certain time the bed reaches a stable state with velocity of the particles equal to zero. Thereafter, the fluid flow is initiated at the inlet. The side walls of the tube are impenetrable and with no-sliping conditions for the fluid. The superficial velocity $\overline{U}$ is imposed as the velocity of the air in the vertical direction at the bottom of the tube, where the velocity gradient of the fluid is zero.

This numerical part is based on Eulerian-Lagrangian method. The fluid flow is solved based CFD with the open source code OpenFOAM (www.openfoam.com), the granular motion is solved with the open source code LIGGGHTS (www.liggghts.com) which is based on DEM, and CFD-DEM coupling is made with the open source code CFDEM (www.cfdem.com). A three dimensional geometry of vertical tube was created and generated a hexahedral mesh with a total number of 38.400 cells. We employed a big particle void fraction model (www.cfdem.com), which is used when the particle is larger than the CFD cells. With the generated mesh, the behavior of the grains inside the fluid flow was well captured (Cúñez and Franklin, 2019). For our CFD-DEM simulations, the single fluid flow is in laminar regime ($Re = O(100)$), so that we considered a laminar regime. In addition, the fluctuations of the particles and the particle-particle interactions are more energetic than the velocity fluctuations of the fluid flow; therefore, the mesh refinement is unnecessary. We run the numerical simulations over 5 seconds for all the cases. For that, each run took approximately 8 to 10 hours to be completed. Finally, all the simulations were performed using a configuration hardware Intel Core i7-4770 3.40GHz with 4 core and 12 GB RAM.

The numerical parameters used in simulations are following: tube diameter $D = 2.5$ mm; number of particles $N = 400$ and $N = 600$; particle diameter $d = 0.5$ mm; particle density $\rho_p = 2500$ Kg/m^3; gas density $\rho_f = 1.2$ Kg/m^3; gas viscosity $\mu_f = 1.8$ kg.m^{-1}s^{-1}; Young's Modulus $E = 0.6$ GPa; Poisson ratio $\sigma = 0.3$; Restitution coefficient $e = 0.9$ Friction coefficient 0.4; time step for CFD 5×10^{-5} s; time step for DEM 1×10^{-6} s. The corresponding parameters of Young's Modulus, Poisson ratio, Restitution coefficient and Friction coefficient were considered based on the studies Tsuji *et al.* (1992); Hoomans *et al.* (1996); Zhou *et al.* (2010).

3. RESULTS

3.1 Fluidized Bed

In this section, we present the results of the main behavior of gas-solid fluidized beds. Figure 1 presents instantaneous snapshots of the bed with $N = 600$ particles and for the two flow rates, $\overline{U} = 1.05$ and $\overline{U} = 1.15$ m/s, respectively. The corresponding times are: $t = 0$, $t = 1$,$t = 1.5$, $t = 2$,$t = 2.5$, $t = 3$, $t = 3.5$, $t = 4$ and $t = 4.5$ seconds.

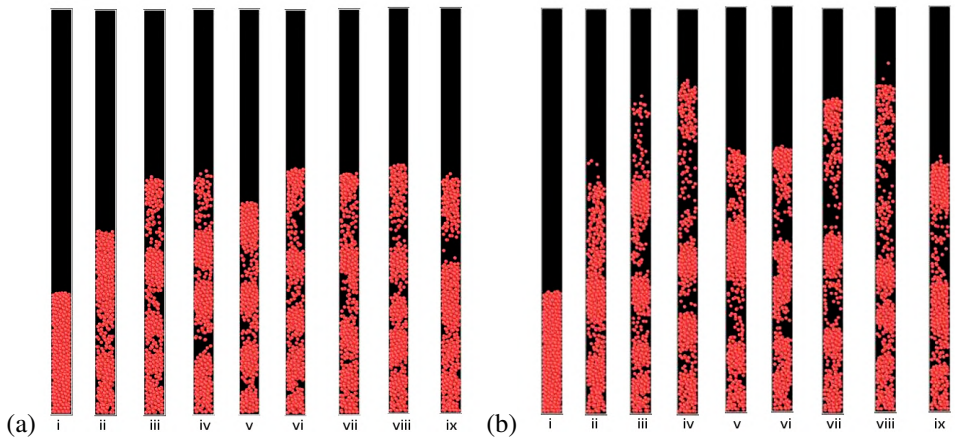

Figure 1. $N = 600$, $\overline{U} = 1.05$ m/s and $\overline{U} = 1.15$ m/s, times i) $t = 0$ s; ii) $t = 1.5$ s; iii) $t = 1$ s; iv) $t = 2$ s; v) $t = 2.5$ s; vi) $t = 3$ s; vii) $t = 3.5$ s; viii) $t = 4$ s; ix) $t = 4.5$ s.

In the simulated conditions, granular plugs and piston bubbles occupying the entire tube cross section were observed in the fluidized bed. These patterns presented almost one-dimensional shape, that propagated upwards and downwards with characteristic lengths and velocities. We have identified and followed each granular plug using numerical scripts in MATLAB. In this way, it was possible to calculate the characteristic lengths of the plugs λ, the upward V_{up} and downward V_{down} velocities of the top of the bed, and the standard deviation of length scale σ_λ, upward velocity $\sigma_{V,up}$, and downward velocity $\sigma_{V,down}$. These data are presented in Tab. 1.

Table 1. Number of particles N, superficial velocity $\overline{U}$, plug upward velocity of the top of the bed V_{up}, plug downward velocity of the top of the bed V_{down}, length scale of plugs λ, length scale of plugs normalized by the grain diameter λ/d, initial bed height h and average height of the fluidized bed h_m, standard deviation of plug upward velocity $\sigma_{V,up}$, standard deviation of plug downward velocity $\sigma_{V,down}$, standard deviation of length scale σ_λ

Case	a)	b)	c)	d)	e)	f)
N	400	400	400	600	600	600
$\overline{U}$ (m/s)	1.05	1.10	1.15	1.05	1.10	1.15
V_{up} (m/s)	0.019	0.032	0.037	0.034	0.052	0.063
V_{down} (m/s)	-0.022	-0.037	-0.044	-0.042	-0.063	-0.083
λ (m)	0.0037	0.0034	0.0031	0.0038	0.0036	0.0035
λ/d	7.38	6.75	6.23	7.56	7.20	6.97
$\sigma_{V_{up}}$ (m/s)	0.0128	0.0192	0.024	0.0176	0.0284	0.0339
$\sigma_{V_{down}}$ (m/s)	0.0155	0.0268	0.0326	0.0281	0.0493	0.0614
σ_λ (m)	0.0013	0.0011	0.0009	0.0013	0.0013	0.0012
$\sigma_{\lambda/d}$	2.68	2.18	1.93	2.55	2.61	2.48
h (m)	0.0101	0.0101	0.0101	0.0149	0.0149	0.0149
h_m (m)	0.017	0.0189	0.0193	0.0275	0.0297	0.0321

The lengths of plugs had a small variations with the initial conditions of the bed, the number of particles N and air superficial velocities $\overline{U}$, and were around $7d$ for all the cases. The characteristic lengths of granular plugs were independent of the initial conditions of the bed.

The velocities V_{up} and V_{down} of the top of the bed presented variations with the initial and boundary conditions of the bed. For N varying from 400 to 600, V_{up} varies from 0.019 m/s to 0.034 m/s for $\overline{U} = 1.05$ m/s and from 0.037 m/s to 0.063 for $\overline{U} = 1.15$. The velocity V_{down} varies from -0.022 m/s to -0.042 m/s for $\overline{U} = 1.05$ m/s and from -0.042 m/s to -0.083 for $\overline{U} = 1.15$. This represents variations of 78% and 70% in V_{up} and 90% and 97% in V_{down} for variations of 50% and 10% in N and $\overline{U}$, respectively.

3.2 Particle Dynamic Motion

In this section, we describe the dynamic behavior of the particles in the fluidized bed. It was analyzed the trajectory and collision of each particle.

The trajectory of each particle was observed with the purpose of verifying how the particles move within and between the plugs formed in the fluidized bed. Considering the characteristic length of each plug, it was possible to establish a criterion to calculate the number of particles that changed plugs. Throughout the trajectory of each particle, it was observed the minimum and maximum height reached in the positive vertical direction z. If the difference between these heights was greater than the characteristic length of the plug λ/d plus three times the standard deviation $\sigma_{\lambda/d}$, then it was established that the particle changed the plug. This behavior can be observed in Fig. 2, the eftmost graphics is Figs 2(a) and 2(b) representing the trajectories of particles that did not change plugs and the other plots the trajectories of the particles that exchange plugs. Table 2 presents some statistics concerning the displacements of individual grains)

For all the beds considered in the simulation, more than 75% of the particles exchange plugs and an increase in superficial velocity $\overline{U}$ caused an increase in the number of particles exchanging plugs. For higher superficial velocities and longer simulation time, 100% of the particles would move along every fluidized bed. Therefore, the number of particles that change plugs depends on the boundary conditions and number of particles N of the bed.

In order to characterize the particle collisions, we observed that after a collision the particle undergoes a great variation in velocity, thus establishing a criterion based on the intensity of the instantaneous acceleration to detect the contact between particles (Aguilar-Corona *et al.*, 2011). This criterion can be verified by comparing the images generated by the simulation and the acceleration graphic as a function of time, the collisions coinciding with the acceleration peaks. It was also observed that the amplitude of the acceleration peaks is always larger in the vertical direction compared to the horizontal component. The Figure 3 shows the components a_x, a_y and a_z of the acceleration of a particle as a function of time t.

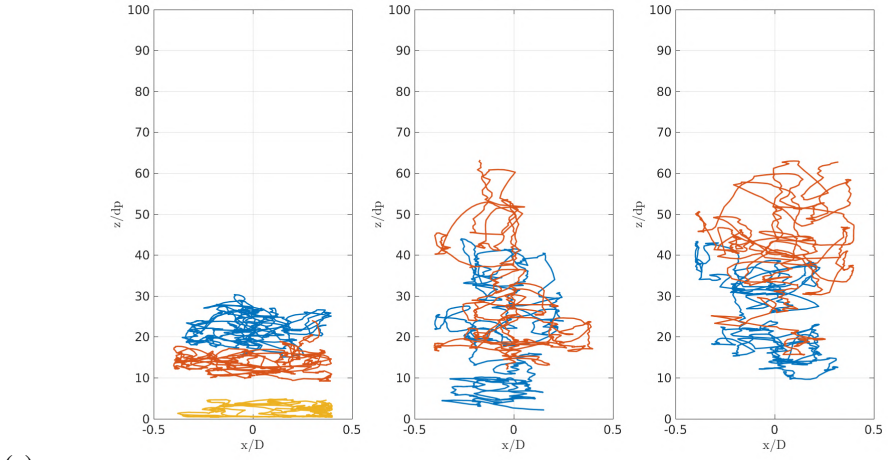

(a)

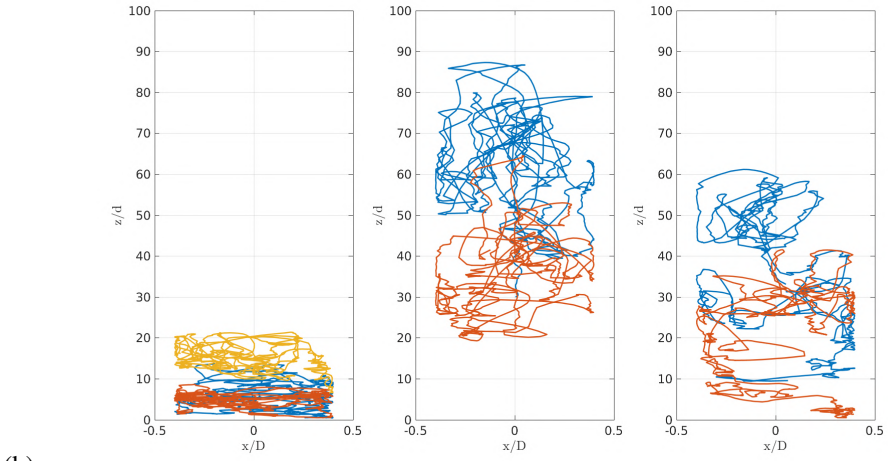

(b)

Figure 2. $N = 600$, (a) $\overline{U} = 1.05$ m/s and (b) $\overline{U} = 1.15$ m/s.

Table 2. Number of particles N, superficial velocity $\overline{U}$, number of particles that changed plugs $\dot{N}_c$, number of particles that not changed plugs $\dot{N}_{nc}$, percentage of particles that changed plugs PN_c, percentage of particles that not changed plugs PN_{nc}, mean distance traveled by grains during a 1s period s_p, standard deviation of distance traveled by grains during a 1s period σ_{sp}.

Case	a)	b)	c)	d)	e)	f)
N	400	400	400	600	600	600
$\overline{U}$ (m/s)	1.05	1.10	1.15	1.05	1.10	1.15
$\dot{N}_c$ (s^{-1})	75.25	91.25	92.5	125	136.75	139.5
$\dot{N}_{nc}$ (s^{-1})	24.75	8.75	7.5	25	13.25	10.5
PN_c	75.25%	91.25%	92.5%	83.33%	91.17%	93%
PN_{nc}	24.75%	8.75%	7.5%	16.67%	8.83%	7%
s_p (m)	0.02985	0.03765	0.04155	0.03672	0.04487	0.05352
σ_{sp} (m)	0.00882	0.01237	0.01425	0.01287	0.0177	0.02165

Let $\vec{a}(t) = (a_x(t), a_y(t), a_z(t))$ be the acceleration of a particle, where $a_x(t), a_y(t)$ and $a_z(t)$ are computed as the time derivative of components of the velocity of particle $\vec{u}_p(t) = (u_x(t), u_y(t), u_z(t))$. Consider

$$A(t) = \left\| \frac{\vec{a}(t)}{g} \right\|$$

with $g = 9.81\ m/s^2$, the acceleration modulus normalized by gravity. In this way, the peaks of the acceleration A coinciding with the particle collision and can be used as a criterion to identify a single collision of a particle. The Figure 4 shows the acceleration of a particle in five seconds of simulation.

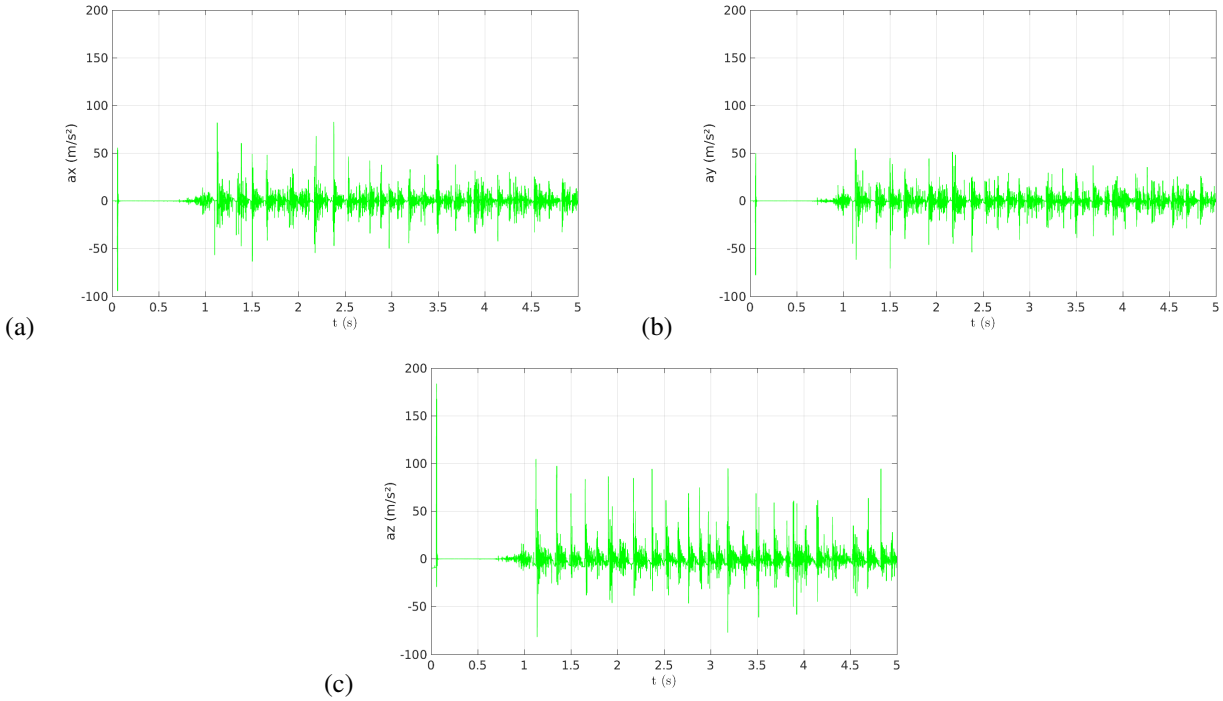

Figure 3. Components of the acceleration of a particle as a function of time t. (a) a_x (b) a_y (c) a_z

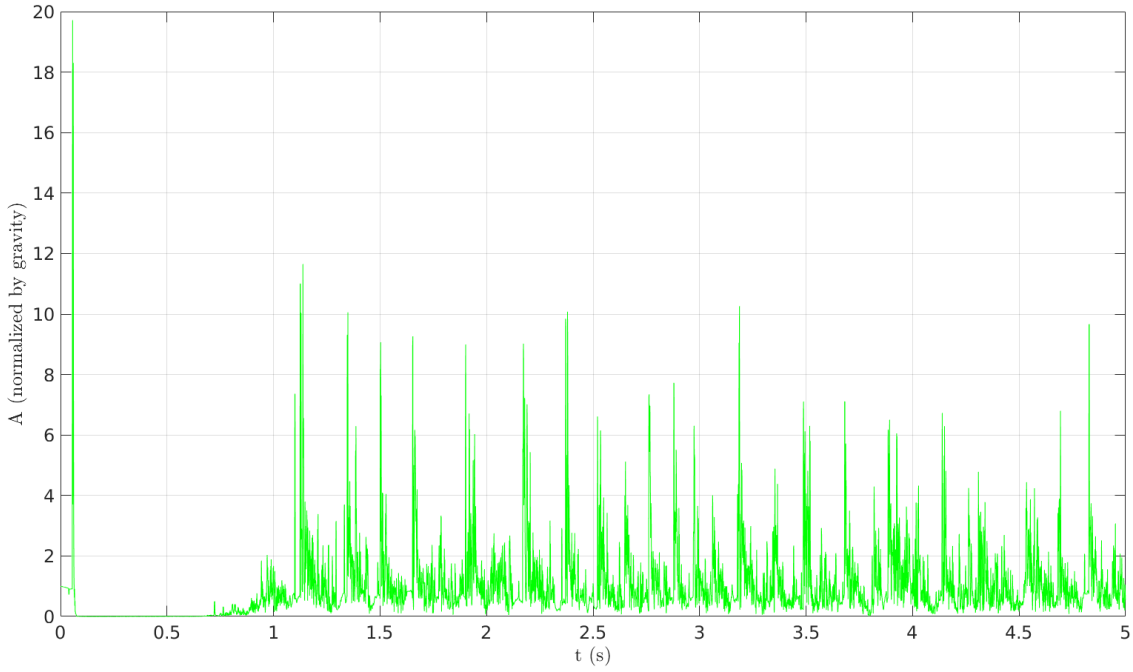

Figure 4. Acceleration normalized by gravity of a particle as a function of time. The peaks of the acceleration represent the collisions particle-wall and particle-particle.

In order to identify the collisions of the particles in numerical simulations, a minimum limit $A = 1$ was established for a peak of acceleration, that is, peaks below that value do not characterize a collision. Comparing the images of the simulation with the plots of A, it is possible to note that particles with acceleration smaller than $A = 1$ are generally falling in regions of high void fractions, in other words, in regions with low particle concentration the acceleration is less than $1g$.

The Figures 5, 6, 7 show the graphics of the acceleration, trajectory and snapshot of the simulation of the collision of a particle with the wall of the tube, respectively. The acceleration and trajectory are shown for time intervals between

$1 < t < 1.45$ and $1.15 < t < 1.35$ seconds, respectively. It is possible to note that the particle begins its trajectory in a plugs, where numerous collisions occur until the particle moves to a region of low-compactness, beginning its fall, where a collision occurs with the wall of the tube and again in fall it reaches and collides with the particles of the region of a plug. The Figure 5 characterizes the acceleration and collision of a particle. In the graph, the accelerations considered

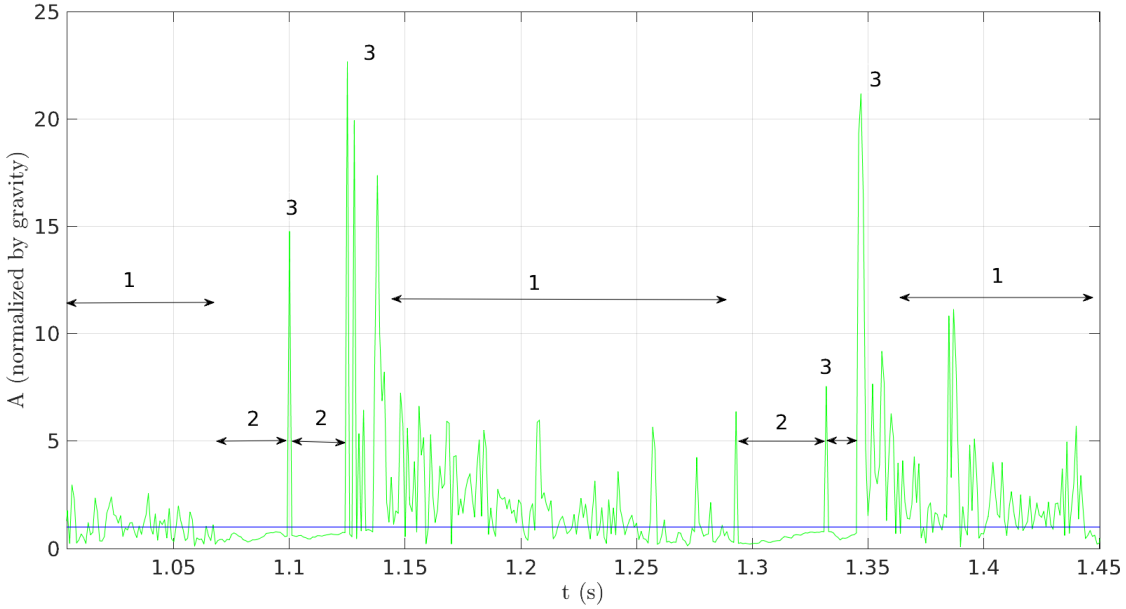

Figure 5. Acceleration normalized by gravity of a particle as a function of time. 1. Particle collisions in the region of a plug, 2. Falling particle, 3. Particle-particle collisions and particle-wall collision.

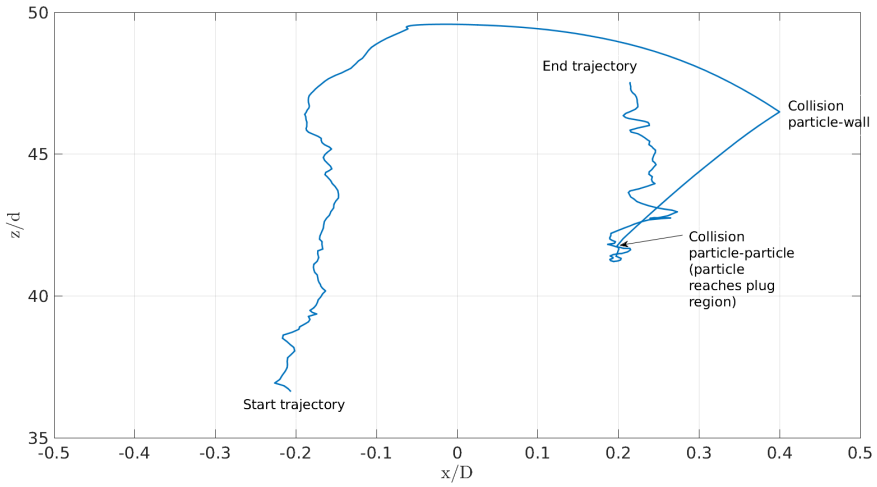

Figure 6. Trajectory of a particle for time interval between $1.15 < t < 1.45$ seconds.

in 1 represent the collisions of particles in plugs or regions of high compactness. The acceleration in 2 represents the fall of a particle from an upper plug to the lower one. These free fall regions are of high void fraction and acceleration of the particulate is generally smaller or near $1g$. At 3, acceleration peaks represent particle collisions falling between plugs that either collide with the wall of the tube, with another falling particle or fall down to strike and collide with a region of high compactness or plug. The trajectory of the particle shown in figure 7 is represented in the graph of figure 6, where it is possible to observe the collision of the particle with the wall of the tube and with a region of high compactness. In Fig. 5, acceleration of the particle corresponds to the time interval between 1.15 and 1.35 seconds.

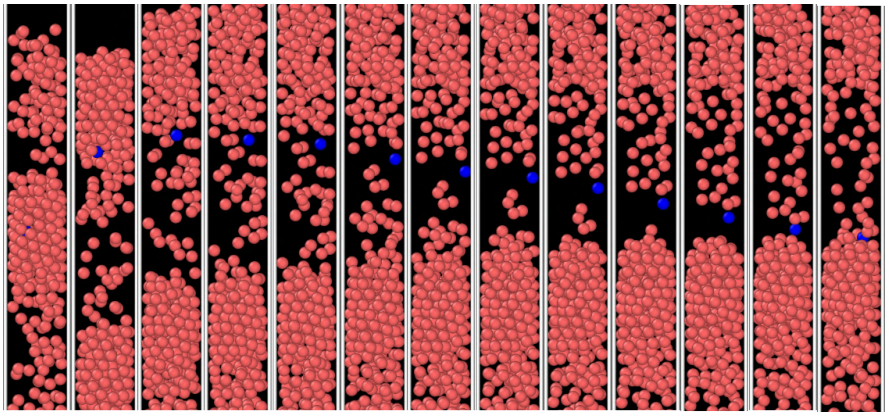

Figure 7. Instantaneous snapshots of the collision of a particle with the wall of the tube. Time interval between $1.2 < t < 1.35$ seconds.

4. CONCLUSIONS

This work investigated numerically a gas-solid fluidized bed in a narrow tube. The confinement effects created by ratio between the tube and grain diameters $D/d = 5$ leads to the formation of alternating high- and low-compactness regions. These regions, known as plugs and piston bubbles, respectively, occupy the entire tube cross section, oscillating upwards and downwards with characteristic lengths and velocities. The collisional phenomena were studied, at the determination of, particle-particle and particle-wall collision was based on the use of a peak acceleration.

The numerical simulations were based on Eulerian-Lagrangian method. We performed three dimensional simulations using a CFD-DEM method with the open source code CFDEM. Two different beds were arranged, consisting of $N = 400$ and $N = 600$ glass beads, and air flows corresponding to cross-sectional mean velocities of $\overline{U} = 1.05$, $\overline{U} = 1.10$ and $\overline{U} = 1.15$ m/s were imposed. We have identified and followed each granular plug in simulations using numerical scripts written in MATLAB, and calculated the characteristic length λ, the upward V_{up} and downward V_{down} velocities of the top of the beds.

The lengths of plugs had small variations and were around $7d$. The velocities V_{up} and V_{down} of the top of the bed presented variations between 0.019 m/s and 0.063 m/s and -0.083 m/s and -0.022 m/s, respectively.

The collisions were detected and characterized in regions of low- and high-compactness. Regions of high-compactness represent the collisions of particles in plugs. In regions of low-compactness represent the fall of a particle from an upper plug to the lower one. This free fall region has high void fraction and the acceleration of the particle is generally smaller or near $1g$.

In this paper, the characteristic lengths of the granular plugs were around $7d$. On the other hand, for the case of liquid fluidized beds in narrow tubes, Cúñez and Franklin (2019) found that the characteristic lengths of the plugs were around $7d$ to $9d$. Both results are similar but further investigation is necessary to draw general conclusions for both cases.

5. ACKNOWLEDGEMENTS

Fernando Cúñez is grateful to FAPESP (Grant no. 2016/18189- 0) and Erick Franklin to FAPESP (Grants No. 2016/13474-9 and No. 2018/14981-7), to CNPq (Grant No. 400284/2016-2) and to FAEPEX/UNICAMP (Grants No. 2210/18 and No. 2112/19) for the nancial support provided. Karlo Rocha is grateful to the IFES-FEM/UNICAMP Dinter.

6. REFERENCES

Aguilar-Corona, A., Zenit, R. and Masbernat, O., 2011. "Collisions in a liquid fluidized bed". *Int. J. Multiphase Flow*, Vol. 37, No. 7, pp. 695 – 705.

Anderson, T.B. and Jackson, R., 1969. "A fluid mechanical description of fluidized beds. Comparison of theory and experiment". *Ind. Eng. Chem. Fundamen.*, Vol. 8, No. 1, pp. 137–144.

Cammarata, L., Lettieri, P., Micale, G. and Colman, D., 2003. "2d and 3d cfd simulations of bubbling fluidized beds using eulerian-eulerian models". *International J. of Chemical Reactor Engineering*.

Cundall, P.A. and Strack, O.D., 1979. "A discrete numerical model for granular assemblies". *Géotechnique*, Vol. 29, No. 1, pp. 47–65.

Cúñez, F.D. and Franklin, E.M., 2019. "Plug regime in water fluidized beds in very narrow tubes". *Powder Technol.*, Vol. 345, pp. 234–246.

Duru, P. and Guazzelli, É., 2002. "Experimental investigation on the secondary instability of liquid-fluidized beds and the formation of bubbles". *J. Fluid Mech.*, Vol. 470, pp. 359–382.

Ghatage, S.V., Peng, Z., Sathe, M.J., Doroodchi, E., Padhiyar, N., Moghtaderi, B., Joshi, J.B. and Evans, G.M., 2014. "Stability analysis in solid-liquid fluidized beds: Experimental and computational". *Chem. Eng. J.*, Vol. 256, pp. 169 – 186.

Gidaspow, D., 1994. *Multiphase flow and fluidization: continuum and kinetic theory descriptions*. Academic press.

Goldschmidt, M.V., Beetstra, R. and Kuipers, J.M., 2002. "Hydrodynamic modelling of dense gas-fluidised beds: Comparison of the kinetic theory of granular flow with 3d hard-sphere discrete particle simulations". *Chemical Engineerin Science*, Vol. 57, pp. 2059–2075.

Hoomans, P.B., Kuipers, M., A., Brierls, W.J. and Van Swaaij, P.M., 1996. "Discrete particle simulation of bubble and slug formation in a two dimensional gas-fluidised bed: a hard-sphere approach". *Chemical Engineerin Science*, Vol. 51, No. 1, pp. 99–118.

Hosseini, S.H., Rahimi, R., Zivdar, M. and Samimi, A., 2009. "Cfd simulation of gas-solid bubbling fluidized bed containing fcc particles." *Korean J. Chem. Eng.*, Vol. 26(5), pp. 1405–1413.

Kafui, K.D., Thornton, C. and Adams, M.J., 2002. "Discrete particle-continuum fluid modelling of gasâĂŞsolid fuidised beds". *Chemical Engineerin Science*, Vol. 57, pp. 2395–2410.

Mahinpey, N., Vejahati, F. and Ellis, N., 2007. "Cfd simulation of gasâĂŤsolid bubbling fluidized bed: an extensive assessment of drag models." *WIT Transactions on Engineering Sciences*, Vol. 56, pp. 51–60.

Tsuji, Y., Tanaka, T. and Ishida, T., 1992. "Lagrangian numerical simulation of plug flow of cohesionless particles in a horizontal pipe". *Powder Technol.*, Vol. 71, No. 3, pp. 239–250.

Wu, G., Ouyang, J. and Li, Q., 2013. "Revised drag calculation method for coarse grid lagrangianâĂŞeulerian simulation of gasâĂŞsolid bubblingfluidized bed". *Powder Technol.*, Vol. 235, pp. 959–967.

Xu, M., Ge, W. and Li, J., 2007. "A discrete particle model for particleâĂŞfluid flow with considerations of sub-grid structures". *Chemical Engineerin Science*, Vol. 62, pp. 2302–2308.

Zenit, R. and Hunt, M.L., 2000. "Solid fraction fluctuations in solid-liquid flows". *Int. J. Multiphase Flow*, Vol. 26, No. 5, pp. 763 – 781.

Zhou, Z.Y., Kuang, S.B., Chu, K.W. and Yu, A.B., 2010. "Discrete particle simulation of particle fluid flow: model formulations and their applicability". *J. Fluid Mech.*, Vol. 661, pp. 482–510.